ISSUE: February 2025

Designing An Open-Source Power Inverter (Part 24): Inverter Output Filter Conundrum

by Dennis Feucht, Innovatia Laboratories, Cayo, Belize

As we approach the end of this Volksinverter design series,[1-23] we address an aspect of power inverter performance that will be critical to commercial implementations of this design for compliance reasons as well as for the proper operation of the equipment being powered. The issue at hand is electromagnetic interference (EMI), and specifically the conducted EMI produced by the inverter (Fig. 1).

The Volksinverter output stage—the inverter itself—has an LC filter. Will it adequately attenuate electromagnetic interference (EMI) currents?

As the question seems straightforward, we might be tempted to turn to simulation for an answer. Indeed, circuit simulation may aid design in general. However, of the four major aspects of power-electronics design—power circuits, magnetics, control, and parasitics—this last aspect of design, in the form of parasitic reactance, poses difficulties when attempting to evaluate the LC filter.

Up to this point in the series, an important reactance associated with the inverter distributed load has been overlooked: the common-mode (CM) capacitance C_{CM} between the distributed power-line output loading the inverter and the Volksinverter ground that completes the CM source loop.

While C_{CM} can be included in a circuit model, we can only estimate its value over a wide possible range, making accurate simulation of LC filter performance difficult. In this part we analyze operation of the LC filter, and discuss different possible solutions to suppression of CM currents, but ultimately settle on a modified configuration of the filter that was presented in part 23. We also analyze how PWM switching sequences affect EMI performance and which sequences are optimal. In the last section, filter design equations are presented for the case with uncoupled inductors. This section includes also some tips on inductor selection based on component choices observed in commercially available inverters.

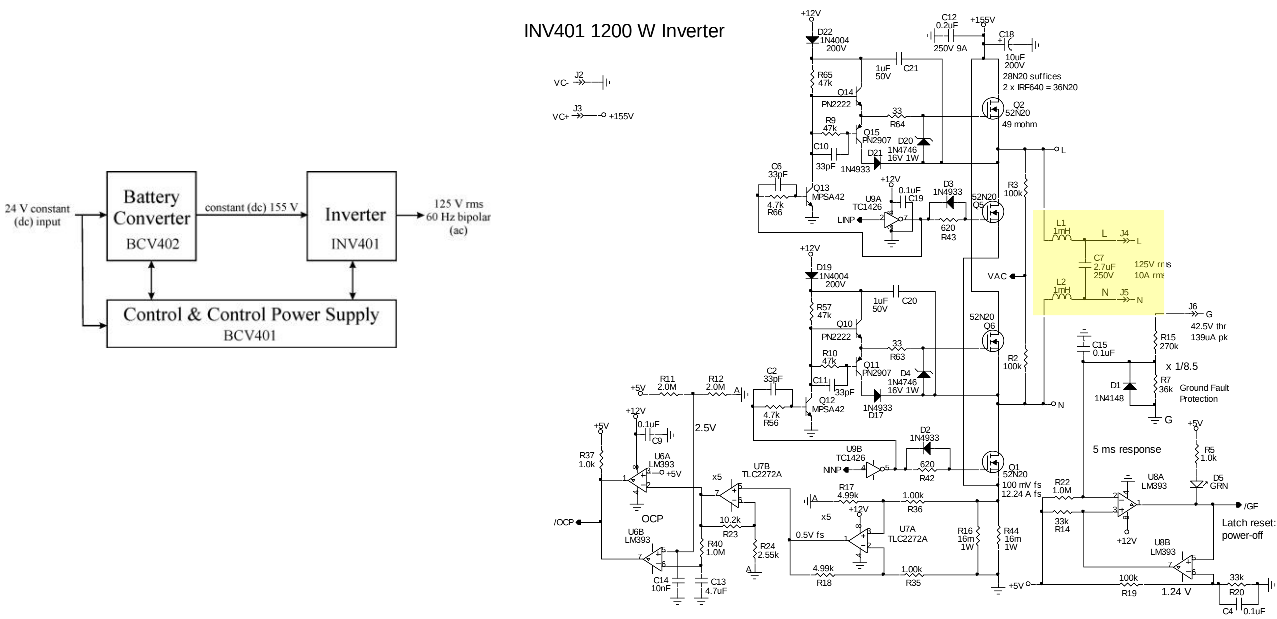

(a) (b)

Fig. 1. Latest version of the INV401 inverter stage with the modified output filter highlighted. The motivation for this modified version of the filter (with uncoupled inductors), which was presented in part 23, is explained below in this part.

Output Common-Mode Noise

The Volksinverter output filter inductor from part 5 (repeated here in Fig. 2) was configured as a coupled inductor for maximum inductance, with the dotted ends of the windings at opposite ends as highlighted in Fig. 3, left. *Differential-mode* (DM) current goes out one terminal and comes back into the other, as shown in Fig. 3, center. Inverter 60-Hz output current is DM but PWM and its harmonics can be both DM and CM.

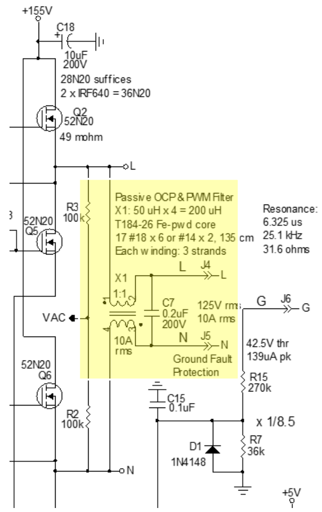

Fig. 2. A section of the inverter output stage showing the original configuration of the output filter with coupled inductors from part 5. Details of this inductor design were discussed further in part 7.

The circuit of Fig. 3, left attenuates PWM harmonics of the output waveform. To maximize inductance, the two windings are configured as a coupled inductor. The 60-Hz line frequency f_g is lower than the inverter switching frequency f_s, and the f_g waveform passes through the filter without attenuation. To filter out PWM harmonics at f_s from the DM power waveform at a fundamental frequency of f_g is an output filter design goal.

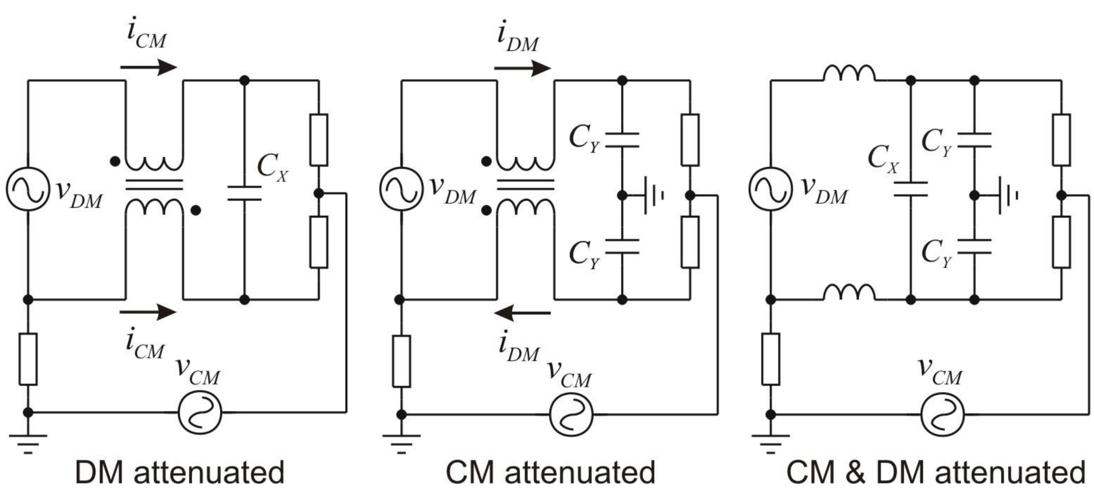

Fig. 3. Left: coupled inductor attenuates PWM DM current but passes CM current; Center: transformer attenuates PWM CM current, bypassing it from output to v_{DM} source, but passes DM current; Right: uncoupled inductors attenuate both PWM CM and DM currents.

However, a minor note is struck in the background music of this article as we turn our attention to *common-mode* (CM) output current, as shown in Fig. 3, left. The CM current loop returning CM current to its H-bridge voltage source of storage capacitor C_o is closed through distributed parasitic capacitance C_{CM}. It develops the average output voltage which is not across power-line loads conducting DM current but floats across the power L and N terminals. It causes i_{CM} through C_{CM} from both output load terminals back to the inverter ground.

In Fig. 3, this parasitic C_{CM} results in EMI voltage v_{CM} at the Volksinverter ground, completing the CM current loop back to the H-bridge input source C_o. A C_Y capacitor from each output terminal provides a return path for CM currents back to the source, bypassing it around the loads. These capacitors are the same in value for maximum CM rejection.

In residential off-grid systems under 10 kW it is not difficult to isolate the solar PV array, battery-bank and charger along with the inverter from the distributed load so that it joins only at the inverter output. Although solar panels might be in electrical contact with their metal supports on the ground or roof where they are mounted, the solar-cell circuits are statically isolated from the frames of the panels. In larger systems (≥ 10 kW), this isolation is more difficult to maintain, leading to H-bridge schemes with isolating off-time switches that prevent PWM CM current to be output by the inverter.

A simple solution to the CM problem is to isolate the inverter output with a 60-Hz transformer—a large, heavy, and costly solution that at any significant power is suboptimal. Consequently, such "boat anchor" designs are largely obsolete, and transformerless circuits have prevailed.

During PWM on-time delivery of load current, the output terminals are driven by what is essentially the H-bridge voltage source V_c across the converter output storage capacitor C_o. During PWM off-time, the H-bridge output terminals are typically shorted by current clamping by the H-bridge MOSFET reverse diodes to either the high or low side of the H-bridge, causing a CM voltage to be applied to the output that can drive C_{CM}.

This DM 0-V output off-time can isolate the output with H-bridge series switches from the C_o source. During PWM on-time, the DM voltage is also applied to C_{CM} but it changes at the output terminals at f_g and is a minor EMI problem.

The Volksinverter four-switch H-bridge output terminals during PWM on-time deliver the desired DM current. During off-time, both low-side switches are on and high-side switches are off. The output terminals become a single low-side node and the transition of one terminal from inverter ground to the C_o high-side node of V_c drives i_{CM} as conducted EMI through C_{CM}, completing the loop back to C_o. If large enough, conducted EMI might even overcurrent power switches.

In the case of H-bridge PWM switching where both high-side switches are on instead of the low-side switches, the voltage transition from off-time to on-time is of opposite voltage polarity as is the resulting i_{CM}. For either of these switch sequencing variants, PWM output attenuation is required. For the existing (described in detail in part 7) Volksinverter design, the output filter is as in Fig. 3, left. It attenuates i_{DM} but passes i_{CM}.

The design modification (as presented above from part 23) uncouples the windings as separate inductors of Fig. 3, right. They must each be doubled in inductance to maintain the same circuit inductance. This uncoupling of the windings sufficiently attenuates i_{CM} to prevent excessive voltage on the power switches and bring common-mode EMI within acceptable levels.

Optimal H-Bridge Switch Sequencing

The present design of Volksinverter H-bridge switch sequencing alternates polarity (POL) and PWM between the half-bridge branches (or "legs") of the H-bridge. INV401 sequencing is labeled 2QU– or "two-quadrant, unipolar off-time with low-side switches on". Multiple switch sequencing alternatives have different EMI consequences and efficiency. Table 1 gives four sequences with both half-cycles of the power output waveform.

Table 1. H-bridge switch sequencing schemes.

Switch Sequence	4Q (FW)	2QB ("hybrid")	2QU–	2QU+
on+	C O O C	C O O C	C O O C	C O O C
off+	O C C O	C C O O	O O C C	C C O O
on–	O C C O	O C C O	O C C O	O C C O
off–	C O O C	O O C C	O O C C	C C O O
+ half-cycle	PWM	POL PWM	POL PWM	PWM POL
– half-cycle	/PWM	POL /PWM	PWM POL	POL PWM

Notes: O = switch open; C = switch conducting; POL = polarity

The full-wave (FW) or four-quadrant sequence is common to high acceleration motor-drives, where active control of off-time current is important for dynamic response. In a power-line inverter it has low EMI but also low H-bridge and filter inductor efficiency.

The two-quadrant bipolar (2QB) scheme shares conduction loss among power switches. The two-quadrant unipolar alternatives have either the low-side switches conducting during off-times (2QU–) or high-side (2QU+). The 2QU± sequences alternate half-bridge legs between half-cycles of POL and PWM. The 2QB sequence dedicates polarity switching (POL) to the left leg while changing PWM and /PWM between output half-cycles on the other leg.

During on-times, DM load current is bipolar and equal in magnitude and tends to cancel fields. During off-times, bridge output terminal voltages are driven by V_c of C_o, and any capacitive path (through C_{CM}) conducts CM current when off-time transitions occur.

Some larger commercial inverters place a switch in series with the bridge that is open during off-time to break any CM current path through the bridge. An alternative is to open all the bridge switches (which breaks the CM loop) and short the output with switches during off-time to provide a filter inductor current path. Half-bridge and multi-level full-bridge schemes have also appeared. For half-bridge circuits, the other leg is a split capacitance with the center-node the neutral (N) output terminal.

Output Filter Design

Each output node of the H-bridge has a series inductance with (uncoupled) inductors. They limit H-bridge load current during the passive OCP interval t_{cd}. The worst case is a load short at the peak output voltage. H-bridge current di/dt is limited by them as is any current into the inverter output from a reactive load. Common-mode current is also impeded by series inductors because they are not magnetically coupled.

The second function of the LC output filter is to attenuate EMI caused by switching harmonics at the output port. An LC filter transfer function decreases asymptotically (or "rolls off") at –2 dec/dec, having two poles, around its resonant frequency f_n. The LC filter transfer function is

$$M(s)=\frac{1}{(s/\omega_n)^2+1} \Rightarrow |M(j\cdot\omega)|=\left|\frac{1}{(j\cdot\omega/\omega_n)^2+1}\right|=\frac{1}{\left|1-\left(\dfrac{\omega}{\omega_n}\right)^2\right|}\ ,\ f_n=\frac{f}{\sqrt{\dfrac{1}{|M(j\cdot\omega)|}-1}}$$

$|M| > 1$ for $f < f_n$ and undamped LC parallel resonance is infinite at f_n. Parasitic resistance in the reactance components makes it finite though still highly underdamped. Filter *damping* depends on load resistance, series resistance in L and C, and *resonant impedance.*

$$Z_n=\sqrt{\frac{L}{C}}$$

Parallel and series resonant damping equations are

$$\zeta_p=\frac{1}{2}\cdot\frac{Z_n}{R},\ \zeta_s=\frac{1}{2}\cdot\frac{R}{Z_n};\ \zeta\equiv 1/2\cdot Q$$

The output load at fs of the INV401 has a resistance of 155 V/12.24 A = 12.7 Ω and the filter is critically damped ($\zeta_p = 1$; no overshoot) by $R = Z_n/2$, where R is the combined series resistance of L and C. The open-load damped LC filter transfer function is an exercise in passive-filter design. Its derivation is a circuit problem left for the reader. The result is

$$M(s)=\frac{s\cdot R_C\cdot C+1}{s^2\cdot L\cdot C+s\cdot(R_C+R_L)\cdot C+1}$$

where R_C and R_L are the parasitic series resistances of C and L. Substitute $s = j\cdot\omega$ and reduce for $|M(j\cdot\omega)|$. Adding load resistance R_o results in a more elaborate transfer function;

$$M(s)=\frac{R_o}{R_o+R_L}\cdot\frac{s\cdot R_C\cdot C+1}{s^2\cdot L\cdot C\cdot\left(\dfrac{R_C+R_o}{R_L+R_o}\right)+s\cdot\left[\dfrac{L}{R_L+R_o}+(R_C+R_L\,\|\,R_o)\cdot C\right]+1}$$

For parasitic component resistances R_L and $R_C \ll R_o$, M reduces to

$$M(s)\approx\frac{s\cdot R_C\cdot C+1}{s^2\cdot L\cdot C+s\cdot[L/R_o+(R_L+R_C)\cdot C]+1},\ R_L,\ R_C \ll R_o$$

The filter must pass the 60-Hz (and 180-Hz third harmonic) power waveform with minimal attenuation while reducing conducted EMI. The output filter design parameters are also constrained by the conducted EMI specification such as the widely used standard for converter EMI: CISPR-22. It specifies its class B (the most stringent) power-line EMI limit at a frequency $f \geq 150$ kHz must not exceed 2 mV.

The attenuation required is 155 V/2 mV = 77500 = 4.89 decades (dec). The LC filter steady-state transfer function rolls off (that is, decreases asymptotically in magnitude) by −2 dec/dec. The PWM harmonic that is 4.89 dec/2 = 2.445 dec above the LC resonant frequency must be below the standard 150-kHz voltage value of 2 mV.

Furthermore, square-wave harmonics k roll off by $1/k$ with frequency, resulting in a reduction in EMI harmonics per decade of −3 dec/dec, and

$$4.89\text{ dec}/3 = 1.63\text{ dec} = 42.66$$

Then the highest allowable $f_n \le (150\ \text{kHz})/10^{1.63} = 150\ \text{kHz}/42.66 = 3516$ Hz. The design constraint is

$$f_n \cdot 10^{1.63} = f_n \cdot (42.66) \le 150\ \text{kHz} \Rightarrow f_n \le 3516\ \text{Hz}$$

In the $M(s)$ transfer function, capacitor series resistance creates a zero in $M(s)$ and reduces attenuation of high-frequency harmonics; hence the need for some EMI margin in the choice of f_n.

The choice of ω_n or f_n must minimize 60-Hz and 180-Hz attenuation but begin to roll off low enough in frequency for EMI attenuation to be within the EMI standard set at 150 kHz. (The 180-Hz third harmonic of the 3HSW power waveform has a smaller amplitude that will be attenuated by < 0.3% relative to the 60-Hz fundamental waveform component.) The INV401 H-bridge square-wave switching frequency is $f_s = 1200$ Hz. By maximizing the allowed f_n, L is minimized. If we set $f_n = 3$ kHz, then $\tau_n = 53.05\ \mu$s, the f_s component passes unattenuated (because $f_n > f_s$), and

$$M(60\ \text{Hz}) = 1.0004\ ;\ L = \tau_n^2/C = 2.814\ \text{ns}^2/C\ \ (\text{ns}^2 = 10^{-9}\cdot\text{s}^2 \ne (10^{-9}\cdot\text{s})^2 = 10^{-18}\cdot\text{s}^2)$$

A choice of 1 mH for each inductor, or a series value of $L = 2$ mH, results in $C = 1.41\ \mu$F. Resonant impedance and reactances are

$$Z_n = 37.70\ \Omega\ ;\ X_L(60\ \text{Hz}) = 754\ \text{m}\Omega \text{ and } -X_C(60\ \text{Hz}) = 1885\ \Omega \Rightarrow i_C(60\ \text{Hz}) = 155\ \text{V}/1885\ \Omega \approx 82.2\ \text{mA}$$

Increasing f_n values reduce both inductor and capacitor values, cost, and size but also do not attenuate the PWM fundamental frequency of 1200 Hz. Although f_s does not cause radio EMI, it is in the audio spectrum and will invariably be heard, coming from iron transformer loads or any component that can transduce it.

To filter f_s, set $f_n < f_s$ to the geometric (logarithmic) mean between $f_g = 60$ Hz and $f_s = 1200$ Hz. Then

$$f_n = \sqrt{f_g \cdot f_s} = 268.3\ \text{Hz} \Rightarrow \tau_n = 593.2\ \mu\text{s} \Rightarrow \tau_n^2 = 351.9\ \text{ns}^2$$

For this value of f_n the resulting $|M(60\ \text{Hz})| = 1.026$ corresponds to a voltage increase at the output of $(1.026)\cdot(155\ \text{V}) = 159$ V. Attenuation of PWM at f_s is $|M(1200\ \text{Hz})| = 0.0526$ or −1.28 dec. A 155-V input to the filter outputs 8.16 V at f_s. The third-harmonic voltage at 3600 Hz is

$$M(j\cdot 3600\ \text{Hz})\cdot(155\ \text{V}) = (5.587\cdot 10^{-3})\cdot(155\ \text{V}) = 866\ \text{mV}$$

and for the fifth harmonic at 6000 Hz is 2.00 mV.

Values for inductance $2\cdot L$ and capacitance C, where L is the value of each of the two inductors, is

$$L = \frac{1}{2}\cdot\frac{\tau_n^2}{C} = \frac{1}{2}\cdot\frac{(1/2\cdot\pi\cdot f_n)^2}{C} = 175.9\ \text{ns}^2/C\ ,\ \ f_n = 268.3\ \text{Hz}$$

If $i_C(60\ \text{Hz})$ is set to 4.1% of the peak fs current of 12.24 A, or 500 mA, then $-X_C = 155\ \text{V}/0.5\ \text{A} = 310\ \Omega$ and

$$C = 8.6\ \mu\text{F} \Rightarrow L = \tfrac{1}{2}\cdot\tau_n^2/C = 175.9\ \text{ns}^2/C \approx 20\ \text{mH}$$

This is a physically large iron-powder core inductor with large wire and a value of L in maximum saturation at 12.24 A fs. A MnZn ferrite core has greater field inductance (per turn^2) with smaller core volume, but the filter inductors would still be quite large.

The key insight is to recognize that $f_s = 1200$ Hz is low enough to not require high-frequency cores; laminated electrical steel is feasible as is found in audio transformers. Iron cores saturate at a magnetic field density that is about a decade higher than that of ferrites as is their field inductance and have an acceptable core loss and size at 1200 Hz. (Another possibility closer to switching magnetics is high-flux material.) With laminated-iron magnetics it is feasible to have an inductor of 20 mH.

Some commercial inverter designs such as the Samlex PSE-24175A have a ferrite inductor while others such as the Pipeman PIUB-3000-24X first-stage filter has two ≈ 2-inch (4.5-cm) OD Fe-pwd-core inductors of 1.07 mH (as measured with an RLC meter at low current) and C = 4.2 μF. The worst-case filter design value of L is at fs current and maximum saturation. The 1.07-mH value will be significantly less—perhaps by as much as half—with $f_n \approx 1.5$ kHz.

In assessing the filter design situation, the passive-OCP limits on L are easily met and the requirement for meeting the conductive EMI standard allows for a range of L and C values, limited by resonant frequency and circulating current i_C(60 Hz) from the value of C. Filter components are minimized in size by setting f_n as high as is allowed by the EMI constraint. In typical commercial inverters, $f_s >> f_g$; in the present INV401 design, $f_s = 20 \cdot f_g = (1.30 \text{ dec}) \cdot f_g$.

The remaining design concern is whether the filter cutoff is steep enough over a 1.30 dec range between f_g = 60 Hz and f_s = 1200 Hz. Is a power distribution system with 8 V of 1200 Hz on the wires acceptable? Commercial sine-wave inverters often have two stages of passive filtering and f_s around 20 kHz with f_n at a higher frequency, resulting in lower values of L and C. A two-stage audio-frequency filter for the INV401 using ribbon iron-core magnetics should be feasible. However, as f_n approaches f_g, an LC filter does not attenuate but amplifies with parallel resonance.

f_n can be made lower than 268.3 Hz if the parasitic resistance of the LC circuit damps the resonance sufficiently but damping also results in power loss. A two-stage LC audio filter can reduce the 1200-Hz component to an acceptable level and is probably the best solution. A two-stage filter transfer function is more difficult to derive and can alternatively be found in the filter literature.

References

1. "Designing An Open-Source Power Inverter (Part 1): Goals And Specifications" by Dennis Feucht, How2Power Today, May 2021.
2. "Designing An Open-Source Power Inverter (Part 2): Waveshape Selection" by Dennis Feucht, How2Power Today, September 2021.
3. "Designing An Open-Source Power Inverter (Part 3): Power-Transfer Circuit Options" by Dennis Feucht, How2Power Today, April 2022.
4. "Designing An Open-Source Power Inverter (Part 4): The Optimal Power-Line Waveshape" by Dennis Feucht, How2Power Today, May 2022.
5. "Designing An Open-Source Power Inverter (Part 5): Kilowatt Inverter Circuit Design" by Dennis Feucht, How2Power Today, July 2022.
6. "Designing An Open-Source Power Inverter (Part 6): Kilowatt Inverter Control Circuits" by Dennis Feucht, How2Power Today, August 2022.
7. "Designing An Open-Source Power Inverter (Part 7): Kilowatt Inverter Magnetics" by Dennis Feucht, How2Power Today, September 2022.
8. "Designing An Open-Source Power Inverter (Part 8): Converter Control Power Supply" by Dennis Feucht, How2Power Today, November 2022.
9. "Designing An Open-Source Power Inverter (Part 9): Magnetics For The Converter Control Power Supply" by Dennis Feucht, How2Power Today, December 2022.
10. "Designing An Open-Source Power Inverter (Part 10): Converter Protection Circuits" by Dennis Feucht, How2Power Today, February 2023.
11. "Designing An Open-Source Power Inverter (Part 11): Minimizing Switch Loss In Low-Input-Resistance Converters" by Dennis Feucht, How2Power Today, March 2023.
12. "Designing An Open-Source Power Inverter (Part 12): Sizing The Converter Magnetics" by Dennis Feucht, How2Power Today, May 2023.
13. "Designing An Open-Source Power Inverter (Part 13): The Differential Boost Push-Pull Power-Transfer Circuit" by Dennis Feucht, How2Power Today, June 2023.

14. "Designing An Open-Source Power Inverter (Part 14): Boost Push-Pull Or Buck Bridge?" by Dennis Feucht, How2Power Today, July 2023
15. "Designing An Open-Source Power Inverter (Part 15): Transformer Magnetic Design For the Battery Converter" by Dennis Feucht, How2Power Today, March 2024.
16. "Designing An Open-Source Power Inverter (Part 16): Transformer Winding Design For the Battery Converter—Efficiency Range And Winding Allotment" by Dennis Feucht, How2Power Today, April 2024.
17. "Designing An Open-Source Power Inverter (Part 17): Transformer Winding Design For the Battery Converter—Alternative Configurations" by Dennis Feucht, How2Power Today, May 2024.
18. "Designing An Open-Source Power Inverter (Part 18): Transformer Winding Design For The Battery Converter—Secondary Winding Design" by Dennis Feucht, How2Power Today, July 2024.
19. "Designing An Open-Source Power Inverter (Part 19): Controller Design For The Battery Converter" by Dennis Feucht, How2Power Today, September 2024.
20. "Designing An Open-Source Power Inverter (Part 20): Converter Inductor Magnetic Design" by Dennis Feucht, How2Power Today, October 2024.
21. "Designing An Open-Source Power Inverter (Part 21): Converter Inductor Winding Design" by Dennis Feucht, How2Power Today, November 2024.
22. "Designing An Open-Source Power Inverter (Part 22): Converter Regulator Dynamics" by Dennis Feucht, How2Power Today, December 2024.
23. "Designing An Open-Source Power Inverter (Part 23): Inverter Driver Design Refinement" by Dennis Feucht, How2Power Today, January 2025.

About The Author

Dennis Feucht has been involved in power electronics for 40 years, designing motor-drives and power converters. He has an instrument background from Tektronix, where he designed test and measurement equipment and did research in Tek Labs. He has lately been working on projects in theoretical magnetics and power converter research.

For further reading on power supply control topics, see the How2Power Design Guide, locate the Design Area category and select "Control Methods".